



U and Th content in magnetite and Al-spinel obtained by wet chemistry and laser ablation methods: implication for (U-Th)/He thermochronometer

5 Marianna Corre¹, Arnaud Agranier², Martine Lanson¹, Cécile Gautheron^{3,1}, Fabrice Brunet¹, Stéphane Schwartz¹

¹ISTerre, Univ. Grenoble Alpes, Univ. Savoie Mont Blanc, CNRS, IRD, Univ. Gustave Eiffel, 38000 Grenoble, France

²UBO, IUEM, Place Nicolas Copernic, 29820 Plouzané, France

³GEOPS, Univ. Paris-Sud, CNRS, Université Paris-Saclay, 91405 Orsay, France

10 *Correspondence to:* Marianna Corre (marianna.corre@univ-grenoble-alpes.fr)

Abstract. Magnetite and spinel thermochronological (U-Th)/He dates obtained in different geological contexts often present significantly dispersed values, that could be related to the low concentration of U and Th isotopes, the lack of standard samples or other parameters. For this purpose, this study focuses on the analysis of U and Th content variability. U and Th in magnetite (natural and synthetic) and in natural Al-spinel samples containing different amounts of U and Th, from 0.02 to 15 116 $\mu\text{g/g}$, are analyzed using both wet chemistry and in-situ laser ablation extraction methods. To increase the number of reference samples, two U-Th doped nanomagnetite powders were synthesized and the U and Th concentration were firstly determined using wet chemistry extraction (U and Th of NMA is $\sim 40 \mu\text{g/g}$ and NMB $\sim 0.1 \mu\text{g/g}$). We show that for both U and Th analyses, the obtained reproducibility of the wet chemistry protocol depends on their concentration and is below 11% for U-Th values higher than $0.4 \mu\text{g/g}$ and reaches 22% for U-Th content lower than $0.1 \mu\text{g/g}$. It implies that (U-Th)/He 20 thermochronological dates cannot be more reproducible than 24% for magnetite containing less than $0.1 \mu\text{g/g}$ of U and Th, explaining part of the natural date variability. Secondly, U and Th concentration extracted by laser ablation on natural magnetite and Al-spinel samples were calibrated using both silicate glass standards and synthetic magnetite samples. The determined U and Th content using NMA sample give similar values than the one obtained by wet chemistry extraction but is 30% overestimated using the glass standard samples. These results highlight the impact of matrix effect on the 25 determination of the U-Th content and we recommend to use a well-characterized magnetite sample for calibrating the U-Th signals by laser ablation. In addition, the scatter on the (U-Th)/He magnetite dates can be expected to be $\sim 20\%$ if the U and Th contents are determined by laser ablation. Such a precision level is not that different to the one obtained using wet chemistry extraction, opening the use the use of laser ablation extraction method for determining (U-Th)/He dates. In the absence of spinel reference for U and Th, the silicate glasses and NMA samples was used for laser ablation calibration and U 30 and Th content and are of $\sim 30\%$ lower compared to values obtained using wet chemistry extraction. This discrepancy



underlines the importance of using a standard with a composition close to that of the mineral of interest. Although magnetite and Al-spinel have related crystal-structures, the magnetite standard is not appropriate for U and Th analysis in Al-spinel.

Key words: (U-Th)/He, magnetite, Al-spinel, wet chemistry, laser ablation, mafic and ultramafic rocks

1 Introduction

35 In the last 15 years, the development of thermochronological (U-Th)/He methods applied to both magnetite (MgHe) and
spinel (SpHe), has opened up new avenues for dating the exhumation of mafic and ultramafic rocks (e.g., Blackburn et al.,
2007; Cooperdock and Stockli, 2016; Cooperdock and Stockli, 2018; Schwartz et al., 2020) and for the chronology of fluid-
rock interactions that produce magnetite through the serpentinization reaction of the mantle with water. (e.g., Cooperdock et
al., 2020; Cooperdock and Ault, 2020). Ultramafic rocks are widely exposed in orogenic and ophiolitic contexts on
40 continents as well as at slow spreading centers, i.e., a couple of thousands of meters under the ocean. Accurate
thermochronological data on ultramafic systems are thus essential to quantify the timing of the exhumation of mantle rocks
in various geodynamic settings, like transform fault in oceanic core complexes or upon the emplacement of ophiolitic units.
Both magnetite, Fe_3O_4 , and spinel *ss*, $(\text{Mg,Fe})(\text{Al,Cr,Fe})_2\text{O}_4$, are iron-bearing oxides which crystallize in the spinel structure
and often incorporate trace amounts of U, Th and Sm (at the ng/g levels) during their crystallization. Helium (He) is very
45 little soluble in minerals (Gautheron and Zeitler, 2020), and only radiogenic He produced during alpha decay of radiogenic
isotopes contained in the mineral structure or from neighbor minerals can accumulate in the crystal structure (e.g., Gautheron
et al., 2022). The (U-Th)/He date acquisition requires the measurement of both radiogenic ^4He on one hand and radioactive
 ^{235}U , ^{238}U , ^{232}Th and ^{147}Sm concentrations on the other hand. Obtained MgHe and SpHe dates for a variety of geological
cases present quite dispersed values in the 5 to 70% range. Such variability could be explained by heterogeneous
50 crystallization timing, variable He diffusion coefficient in those minerals, alpha-implantation from neighboring U-Th-rich
mineral or associated with the very low U, Th and Sm content in those minerals (e.g., Cooperdock and Stockli, 2016;
Cooperdock and Stockli, 2018; Schwartz et al., 2020; Gautheron et al., 2022), which is therefore difficult to measure
precisely. In addition, well-characterized magnetite and spinel samples as well as a collection of systematic analyses of U
and Th precision and error for samples having different U and Th concentrations, are lacking for the generalization of this
55 emerging dating method. The accurate determination of Sm contents will be not discussed here because Sm is routinely
analyzed, and it contributes to only 0.0012% of the ^4He budget (Cooperdock et al., 2019).
In this contribution, we analyzed U and Th in samples of various origins, e.g., natural and U-Th doped home-made synthetic
magnetite as well as natural Al-spinel, which display a range of U and Th concentrations, to determine the possible range of
analytical dispersion. Firstly, a wet-chemistry extraction with isotopic dilution method and U and Th analysis using an
60 Inductively Coupled Plasma Mass Spectrometer (ICP-MS) has been performed. The latter is similar to the one proposed
Blackburn et al. (2007) and Cooperdock and Stockli (2016). In parallel, we explored in-situ quantification of U and Th



concentrations in magnetite and Al-spinel by Laser Ablation (LA) extraction coupled to Inductively Coupled Plasma Mass spectrometer (LA-ICP-MS). The latter method, however, requires the use of appropriate solid standards with matrix effects similar to those affecting the samples of interest (e.g., Steenstra et al., 2019; Koch et al., 2002). The obtained LA-ICP-MS results were calibrated using silicate glass standards, and also by using, in addition, a home-made synthetic U-Th magnetite. The reproducibility, accuracy, and applicability of both methods are discussed along with their impact on the determination of (U-Th)/He dates.

2 Methods

2.1 Samples and synthesis characterizations

To test the precision of the wet chemistry analysis, we analyzed the U and Th contents in (1) iron oxide with silicates assemblage which is commonly used as standard for major elements (IF-G) (number of analyzes $n = 15$), (2) natural magnetite ($n = 17$) and natural spinel ($n = 14$), and (3) two doped U-Th synthetic magnetite samples of well-defined U and Th contents ($n = 16$ and 12). A description of the samples is reported in Table 1.

2.1.1 Natural samples

Three natural samples were selected for this study, a magnetite-bearing standard (IF-G), magnetite single-crystals (RB) from an alpine ophiolite and a purchased aluminous spinel crystal. The IF-G sample is a mixture of magnetite, quartz and actinolite (Govindaraju, 1995), sampled from a large iron-ore deposit of the Issua supracrustal belt, West Greenland, that is used as a standard for major elements (Govindaraju, 1995). Reported U and Th concentrations in this sample from 9 independent studies range from 0.01 to 0.03 $\mu\text{g/g}$ and 0.03 to 0.1 $\mu\text{g/g}$ respectively (Govindaraju, 1995; Dulski, 2001; Bolhar et al., 2004; Kamber et al., 2004; Guilmette et al., 2009; Parks, 2014; Bolhar et al., 2015; Viehmann et al., 2016; Table 1). The second sample (RB) is made of millimeter-sized magnetite crystals sampled in the Rocher Blanc ophiolite (western Alps, France; Tricart and Schwartz, 2006) that was already studied for MgHe thermochronology by Schwartz et al. (2020). The U and Th contents of the RB euhedral magnetite are in the 0.006 to 0.029 $\mu\text{g/g}$ range (Table 1). Finally, a 5 cm large crystal of aluminous spinel (Al-Spl), $(\text{Mg}_{0.65}\text{Fe}_{0.35})\text{Al}_2\text{O}_4$, of unknown origin was obtained from a jewelry store and selected because of its size and purity (Table 1).

2.1.2 U-Th doped synthetic magnetite samples

Two batches of U-Th doped nanomagnetite powder (NMA and NMB) were obtained by co-precipitation from FeCl_2 and FeCl_3 solutions (Martínez-Mera et al., 2007). Equal amounts of U and Th, $\sim 40 \mu\text{g/g}$ for NMA and $\sim 0.05 \mu\text{g/g}$ for NMB were added to the acidified FeCl_2 starting solution. All solutions were prepared using boiled de-ionized water (MilliQ, 18.2 MOhms), deoxygenated by bubbling with N_2 gas for 30 min. Instantaneous precipitation of magnetite was achieved at 45°C by simultaneous addition of the 0.125 mol/L of FeCl_2 and FeCl_3 solutions to an ammonia solution at 0.2 mol/L. The solid



was then separated from the supernatant using a permanent magnet and it was rinsed four times with oxygen-free MilliQ water to avoid oxidation. X-ray powder diffraction indicated the production of 85% of magnetite and 15% of goethite and allowed to estimate the grain size to 15 nm from the diffraction peaks width. Complementary experiments were performed to determine the U and Th host phase(s) in the nanomagnetite product, which are presented in the Appendix A.

Table 1. Samples description.

Sample	Issua magnetite-quartz (IF-G)	Rocher Blanc Magnetite (RB)	Aluminous spinel (Al_Spl)	Nanomagnetite powder A (NMA)	Nanomagnetite powder B (NMB)
Origin	Issua belt (Greenland)	Rocher Blanc ophiolitic massif (French Alps)	Unknown	Synthetic	Synthetic
Physical characteristics	Powder of 50 μm (53 vol.% of quartz, 37 vol.% of magnetite and 10 vol.% of actinolite).	Euhedral and pseudo-euhedral single crystals (400 to 600 μm across)	Single crystal (5 cm)	15 nm powder (85 vol.% magnetite and 15 vol.% of goethite)	15 nm powder (85 vol.% magnetite and 15 vol.% of goethite)
Chemical characteristics	U ($\mu\text{g/g}$): 0.013 to 0.03 Th ($\mu\text{g/g}$): 0.03 to 0.1 $\mu\text{g/g}$	U ($\mu\text{g/g}$): 0.008 to 0.029 Th ($\mu\text{g/g}$): 0.006 to 0.020 n =7; Schwartz et al. (2020)	U, Th, Sm ($\mu\text{g/g}$): unknow	U expected concentration: 40 $\mu\text{g/g}$ Th expected concentration: 40 $\mu\text{g/g}$	U expected concentration: 0.05 $\mu\text{g/g}$ Th expected concentration: 0.05 $\mu\text{g/g}$
Preparation for LA-ICP-MS analysis	Due to the mineral heterogeneity even after grinding IF-G was not analyzed by LA-ICP-MS	Grinding with a planetary mill in a 150 mL agate bowl with 10 agate beads of 10 mm diameter, 2 grams of magnetite and 100 mL ethanol for 2 \times 10 min at 500 rpm 40 mg of powder is pressed at ~1000 MPa (20000 N) to have pellet with a diameter of 5 mm. Pellets are embedded in epoxy		40 mg of powder is pressed at ~1000 MPa (20000 N) to have pellet with a diameter of 5mm. Pellets are embedded in epoxy	

2.2 Sample preparation for U and Th analysis

For the RB magnetite and the spinel sample (Al_Spl), 2 grams of material were ground in a planetary mill at 500 rpm for 10 min to obtain a grain size of ~2 microns. Samples NMA and NMB which already consisted in a nano-particle powder did not necessitate grinding. The U and Th contents of these 4 samples were retrieved using wet chemistry and laser ablation and analyzed with ICP-MS. Pellets were obtained from 40 mg of powder using a pressure of ~1000 MPa (20000 N) into 5 mm diameter pellets and embedded in epoxy resin. The IF-G sample that could not be pelletized due to the heterogeneous size of the minerals forming the mixture after grinding. This size heterogeneity can also lead to a nugget effect on LA-ICP-MS analysis.



2.3 Wet chemistry

2.3.1 Sample digestion

Every step of the sample preparation was conducted in a Class 10000 clean laboratory at Institut Universitaire Européen de la Mer (IUEM, France), using deionized water obtained on a Millipore® Milli-Q system set at resistivity of 18.2 MΩ, and sub-boiled acids. Sample digestions and purification were performed for magnetite and spinel in a 2 mL Savilex® Teflon microbombs. Vials were pre-washed using a sequence of purified nitric acid (HNO₃) and a fluoridric acid (HF)-nitric acid (HNO₃)-perchloric acid (HClO₄) mixtures at 120°C.

About 0.005 to 0.1 g of IF-G, RB, Al_Spl and synthetic nanomagnetite NMA and NMB powder samples were dissolved with ~10 µL of a 4.49 ng/g and 3.67 ng/g in-house ²³⁵U and ²³⁰Th mixed spike (Gautheron et al., 2021), in 2 mL Savilex® microbombs. For both magnetite and aluminous spinel, we used for the digestion protocol, a mixture of 1.5 mL aqua regia (1 volume of 10.5 N HCl + 3 volumes of 18N HNO₃) + 0.5 mL of 29N HF+ 2 drops of concentrated HClO₄. Even though aqua regia was itself, sufficient to ensure the total dissolution of magnetite (Blackburn et al., 2007), HF was added, in order to get rid of possible silicate nano-inclusions. The purpose of HClO₄ (evaporation temperature above 180°C) was simply to inhibit the trapping of rare earth elements in fluoride crystals during evaporation (e.g., Li and Lee, 2006; Inglis et al., 2018; Ilyinichna et al., 2020). For magnetite, the acid digestion at 130 °C took only a couple of hours, but acids were evaporated after a minimum of 24h, following two steps: 1) 130 °C until HCl, HNO₃ and HF was evaporated; and then 2) 180 °C to evaporate HClO₄. At the end we obtained a solid residue, and we added 0.5 mL of 1N HNO₃ before closing the microbombs and placing them on a hot plate at 100 °C.

Spinel is a refractory mineral and requires a more aggressive treatment to get fully dissolved. The digestion is possible in the same acid mixture as for magnetite. However, digestion was carried out within 2 mL Savilex® Teflon microbombs, sealed with a wrench top closure and Ultem® sockets (Inglis et al., 2018) in order to increase the temperature into the vial. The temperature is set at 130 °C for at least a week, and for some aliquots, this dissolution has been repeated up to three times before complete dissolution.

2.3.2 U and Th dilution

After digestion, the solutions were diluted to reach suitable concentrations of Fe (<1500 µg/g) for HR-ICP-MS analysis. The quantitative determination of U-Th abundances can therefore hardly be led on too diluted solutions, i.e., with dissolution factors >3000, as it is routinely proposed for silicate rocks/minerals, e.g., Li and Lee (2006). However, magnetite is made of >75 wt.% Fe, and spinel contain ~25 wt.% Fe and up to ~50% Al. The direct analyze of undiluted magnetite/spinel solutions, loaded with these three elements by ICP-MS, is known to induce strong non-spectroscopic (or “matrix”) effects on both introduction and ionization (Koch et al., 2002; Steenstra et al., 2019).



2.4 Analytical conditions

2.4.1 Wet chemistry extraction and U and Th analysis

U and Th analyses were performed on ICP-MS Thermo® Element XR at IUEM associated to either a PFA nebulizer
140 connected to a standard quartz cyclonic chamber or a nitrogen-supplied desolvating nebulizer (ESI® apex Q Elemental
Scientific) introduction system (Potin et al., 2020; Costa et al., 2020), depending on the required level of sensitivity. Isotope
dilution analyzes are made possible by the ^{235}U and ^{230}Th mixed spike additions operated before the sample digestion. In
addition, to the U, Th elements, the Mn content (^{54}Mn isotope) was additionally measured.

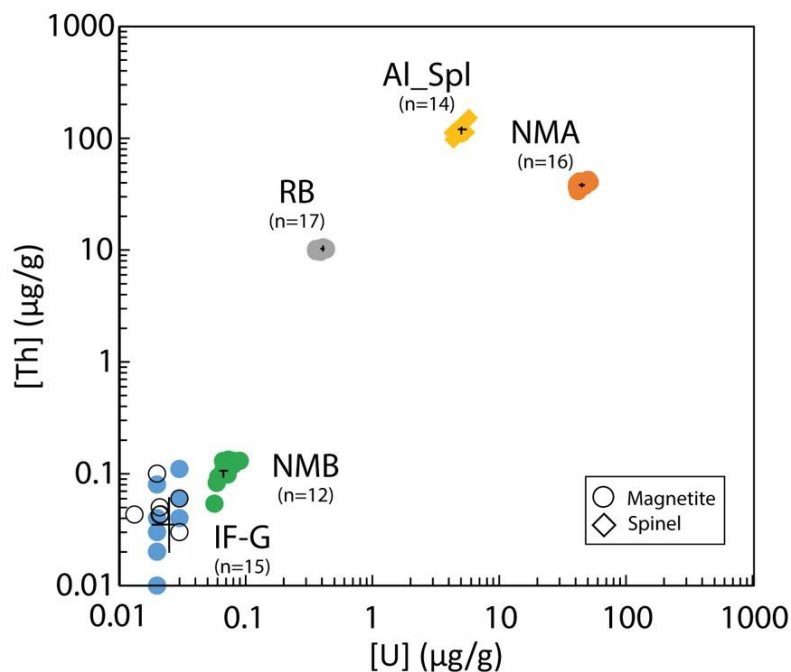
2.4.2 In situ laser ablation extraction and U and Th analysis

145 In-situ LA-ICP-MS analyses were performed on pellets-using a Compex Pro102 Coherent Laser Ablation System coupled to
an ICP-MS Thermo® Element XR at IUEM (e.g., VanKooten et al., 2019; Kubik et al., 2021) operated in its low resolution.
The laser has a directional power maintained at 1200 W, it emits at the wavelength of 193 nm (Ar-F type) and has pulse
duration in the nanosecond range. The energy output was set at 20 J/cm², with a laser frequency of 10 Hz. The spot
diameters, comprised between 90 and 160 μm, were adapted depending on the U and Th contents of the targeted pellets (RB,
150 NMA, Al_Spl). Gas blanks were systematically checked by running 10 cycles of measurements before igniting the laser. The
whole surface of pellets was covered by ten LA-ICP-MS analyzes, each one of them consisted in 30 measurements. In
addition, the Mn content (^{54}Mn isotope) was measured with the wet chemistry method by ICP-MS to be used as an internal
standard for the ablated mass. The calibration was originally operated using silicate international glass standards, BHVO-2g,
BIR1g and BCR2g (Gao et al., 2002), and complemented with the NMA nanomagnetite sample.

155 3 Results

3.1 Wet chemistry U and Th concentration results

The range of the U and Th concentrations obtained by wet chemistry method are reported in Figure 1 and Table 2. U and Th
concentrations range from 0.02±0.01 to 45.62±3.40 μg/g and from 0.04±0.03 to 116.01±12.60 μg/g respectively. One can
notice that the U and Th contents measured in this study for the RB sample differ by a factor ~100 from the one obtained by
160 Schwartz et al. (2020). We assume that the sample powder was accidentally contaminated with U and Th during the
preparation, leading to homogeneous richer U and Th content than expected (Table 2). This powder is still analyzed in this
study because the U and Th is homogeneous.

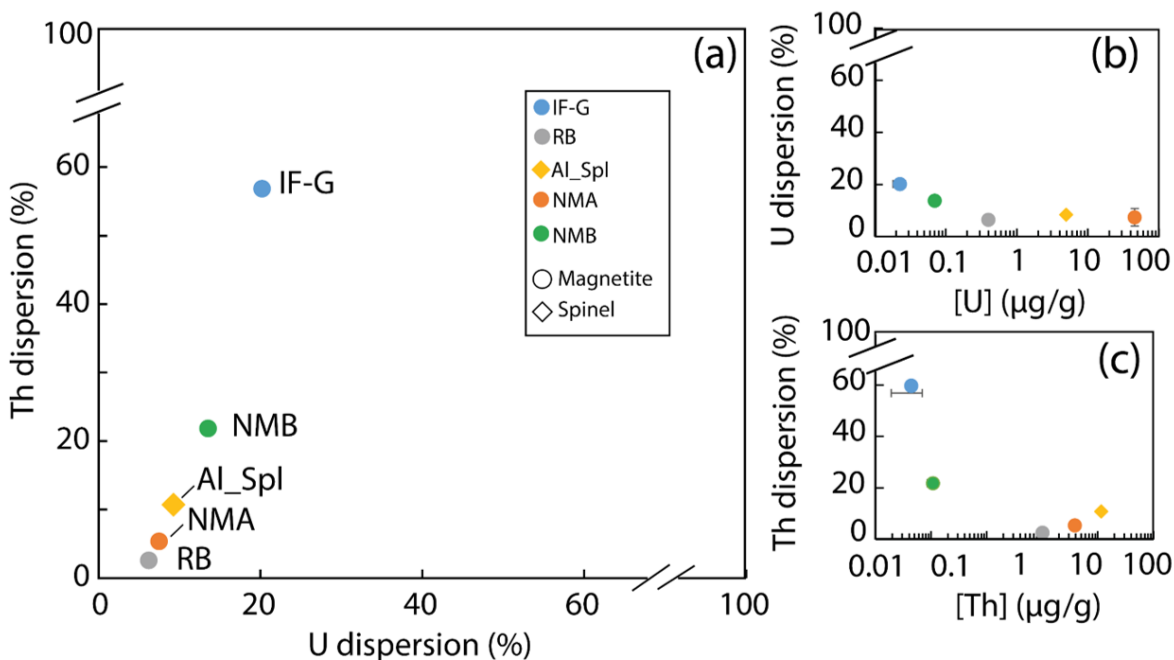


165 **Figure 1.** U and Th content obtained by wet chemistry extraction and associated mean value and standard deviation (black cross), black empty circles represent IF-G results from the literature (Govindaraju, 1994; Govindaraju, 1995; Dulski, 2001; Bolhar et al., 2004; Kamber et al., 2004; Guilmette et al., 2009; Parks et al., 2014; Bolhar et al., 2015; Viehmann et al., 2016).

The U and Th concentration shows some scattering that seems to evolve with the concentration. Figure 2a shows this dispersion in % (i.e., coefficient of variation, which is the standard deviation divided by the mean times 100) of the measured U and Th concentrations for each sample, reported at 1 sigma. The dispersion is more important for Th than for U, whatever the sample. The two samples showing the lower U and Th concentrations, i.e., IF-G and NMB, are those having the most scattered values, 20.2% and 13.8% for U, respectively, and 56.8% and 21.8% for Th, respectively (Figures 2a, b and c). The U and Th content obtained for the IF-G sample is similar to the one obtained in former studies: U concentration ranges from 0.013 to 0.03 $\mu\text{g/g}$ and Th concentration ranges from 0.03 to 0.1 $\mu\text{g/g}$ (Govindaraju, 1995, Dulski, 2001; Bolhar et al., 2004; Kamber et al., 2004; Guilmette et al., 2009; Parks et al., 2014; Bolhar et al., 2015; Viehmann et al., 2016; Fig. 1). The dispersion by 20.2% and 56.8% for the U and Th content for IF-G is comparable with dispersion obtained in these literature data. For the RB, Al_Spl and NMA samples, the dispersion of U content in present similar values that range between 6.5% and 8.4%, the dispersion of Th content is higher for NMA and Al_Spl than for RB of lower concentration (i.e., NMA: 5.4%; Al_Spl: 10.9%; and RB: 2.6%).

170

175



180 **Figure 2.** (a) Dispersion of the U and Th content obtained by wet chemistry extraction. (b) and (c) Mean U and Th content as a function of the associated dispersion respectively.

Table 2. U and Th concentration results obtained by wet chemistry extraction.

Samples	U (μg/g)	±1σ	Th (μg/g)	± 1σ
IF-G				
IF-G 1	0.03	0.0002	0.06	0.0003
IF-G 2	0.03	0.0002	0.06	0.0007
IF-G 3	0.02	0.0004	0.03	0.0003
IF-G 4	0.02	0.0001	0.03	0.0004
IF-G 5	0.02	0.0002	0.04	0.0005
IF-G 6	0.02	0.0002	0.03	0.0002
IF-G 7	0.02	0.0001	0.04	0.0002
IF-G 8	0.02	0.0001	0.03	0.0003
IF-G 9	0.03	0.0001	0.04	0.0003
IF-G 10	0.02	0.0001	0.04	0.0002
IF-G 11	0.02	0.0001	0.04	0.0002
IF-G 12	0.02	0.0001	0.08	0.0003
IF-G 13	0.02	0.0001	0.02	0.0005
IF-G 14	0.03	0.0002	0.11	0.0015
IF-G 15	0.02	0.0002	0.01	0.0005
	Mean (μg/g)	± coeff. of variation %	Mean (μg/g)	± coeff. of variation %
IF-G	0.02	20.2	0.04	56.8
Rocher Blanc				
RB 1	0.36	0.002	10.20	0.05
RB 2	0.43	0.003	10.28	0.14
RB 3	0.42	0.002	10.27	0.05
RB 4	0.39	0.001	9.97	0.05



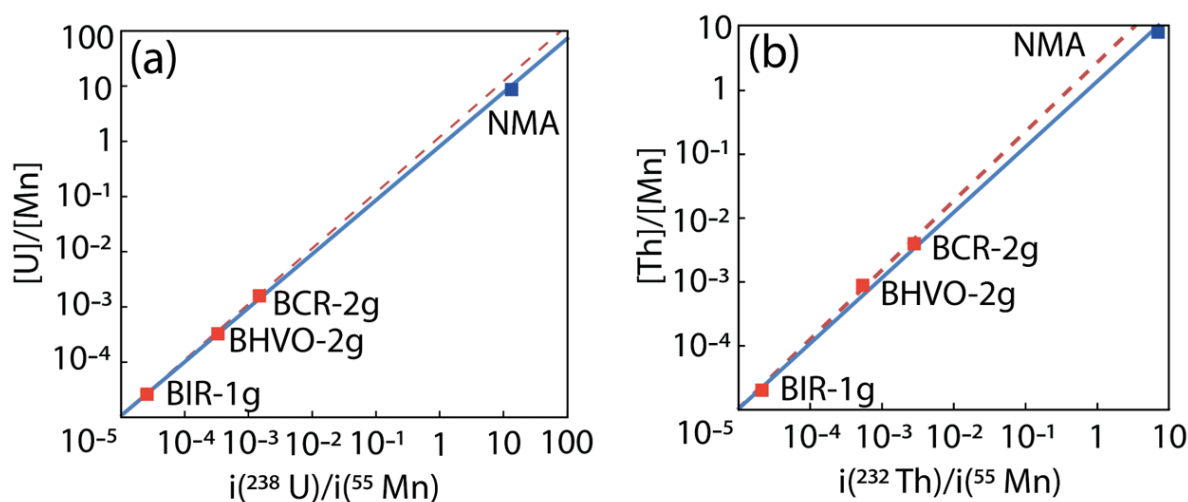
RB 5	0.43	0.002	10.08	0.04
RB 6	0.41	0.002	10.54	0.05
RB 7	0.42	0.001	10.28	0.05
RB 8	0.42	0.001	10.17	0.04
RB 9	0.42	0.002	10.30	0.03
RB 10	0.41	0.002	10.15	0.04
RB 11	0.40	0.001	10.43	0.03
RB 12	0.39	0.001	10.37	0.03
RB 13	0.36	0.001	9.76	0.03
RB 14	0.38	0.001	10.21	0.04
RB 15	0.39	0.003	9.60	0.04
RB 16	0.36	0.002	9.77	0.04
RB 17	0.36	0.002	9.90	0.04
	Mean (µg/g)	± coeff. of variation %	Mean (µg/g)	± coeff. of variation %
RB	0.40	6.5	10.13	2.6
Aluminons spinel				
Al_Spl 1	5.04	0.03	109.25	1.11
Al_Spl 2	4.93	0.07	113.81	1.53
Al_Spl 3	5.03	0.03	113.58	0.98
Al_Spl 4	5.18	0.07	109.85	0.92
Al_Spl 5	5.19	0.03	110.26	0.71
Al_Spl 6	4.96	0.04	113.20	1.00
Al_Spl 7	5.46	0.05	112.88	0.57
Al_Spl 8	4.36	0.04	97.11	0.71
Al_Spl 9	4.89	0.03	116.70	1.81
Al_Spl 10	5.77	0.10	151.96	1.13
Al_Spl 11	4.50	0.02	116.44	0.62
Al_Spl 12	4.49	0.02	115.54	0.57
Al_Spl 13	4.30	0.03	111.78	0.06
Al_Spl 14	5.08	0.02	131.84	0.74
	Mean (µg/g)	± coeff. of variation %	Mean (µg/g)	± coeff. of variation %
Al_Spl	4.94	8.4	116.01	10.9
Nanomagnetite A				
NMA 1	50.52	0.44	42.26	0.23
NMA 2	49.48	0.91	39.84	0.17
NMA 3	51.98	0.67	40.40	0.19
NMA 4	47.32	0.44	37.26	0.16
NMA 5	41.87	0.42	33.49	0.17
NMA 6	45.67	0.58	38.29	0.19
NMA 7	48.01	0.25	39.19	0.16
NMA 8	46.96	0.59	37.90	0.16
NMA 9	47.48	0.80	37.84	0.15
NMA 10	42.85	0.18	37.84	0.10
NMA 11	41.06	0.27	36.38	0.09
NMA 12	43.53	0.09	39.81	0.11
NMA 13	45.95	0.19	40.25	0.10
NMA 14	42.71	0.20	40.60	0.18
NMA 15	43.13	0.27	40.89	0.25
NMA 16	41.34	0.26	39.25	0.26
	Mean (µg/g)	± coeff. of variation %	Mean (µg/g)	± coeff. of variation %
NMA	45.62	7.4	38.84	5.4
Nanomagnetite B				



NMB_1	0.07	0.0003	0.13	0.001
NMB 2	0.06	0.0002	0.09	0.001
NMB 3	0.07	0.0003	0.13	0.001
NMB 4	0.07	0.0004	0.11	0.001
NMB 5	0.07	0.0005	0.11	0.001
NMB 6	0.07	0.0004	0.11	0.001
NMB 7	0.07	0.0004	0.10	0.001
NMB 8	0.06	0.0003	0.05	0.001
NMB 9	0.06	0.0003	0.08	0.001
NMB 10	0.08	0.0010	0.13	0.001
NMB 11	0.08	0.0005	0.12	0.001
NMB 12	0.09	0.0005	0.13	0.001
	Mean (µg/g)	± coeff. of variation %	Mean (µg/g)	± coeff. of variation %
NMB	0.07	13.8	0.11	21.8

3.2 In-situ U and Th concentration results

185 To calculate the U and Th concentration from LA-ICP-MS signal, we used the U/Mn and Th/Mn ratios given for silicate
 glass standards and the mean value obtained using wet chemistry for the NMA sample and the LA-ICP-MS signal
 $i(^{238}\text{U})/i(^{55}\text{Mn})$ and $i(^{232}\text{Th})/i(^{55}\text{Mn})$ for the silicate glasses and NMA samples. Thus, for NMA sample, we assume that the
 mean U and Th concentrations obtained by wet chemistry method were accurate enough to be used. The U/Mn and
 $i(^{238}\text{U})/i(^{55}\text{Mn})$ data or the Th/Mn and $i(^{232}\text{Th})/i(^{55}\text{Mn})$ data for each silicate glass samples are well aligned as shown on
 190 Figure 3 (dotted red line). The results for the NMA sample are slightly shifted from the silicate glass calibration lines, and a
 second calibration was performed using all results (silicate glass and NMA) that reported on Figure 3 (blue line). Using those
 calibration in mind, we calculate the U and Th concentrations for the RB sample using silicate glass standards ($U = 0.5 \pm 0.1$
 and $Th = 14.7 \pm 2.4 \mu\text{g/g}$) and using silicate glasses and NMA samples ($U = 0.4 \pm 0.1$ and $Th = 10.4 \pm 1.7 \mu\text{g/g}$) (Table 3).
 Similarly, U and Th concentrations in Al_Spl were determined by LA-ICP-MS using silicate glass standards, yielding U and
 195 Th concentration of respectively 4.1 ± 0.5 and $88.8 \pm 8.6 \mu\text{g/g}$ (Table 3) and including NMA sample leading to concentration
 of 4.0 ± 0.5 and $79.2 \pm 7.7 \mu\text{g/g}$ for U (Table 3, Fig. 3).



200 **Figure 3.** Calibration lines used for the calibration of the LA-ICP-MS signal. **(a)** U/Mn-calibration lines using silicate glass standards (dotted red line) and NMA nanomagnetite sample (blue line). **(b)** Th/Mn calibration lines with silicate glass standards (dotted red line) and NMA nanomagnetite sample (blue line).

Table 3. U and Th concentration determined using LA-ICP-MS method with two types of calibration (silicate glasses only and silicate glasses plus NMA sample).

	U (µg/g)	±1σ	Th (µg/g)	±1σ
Glass standards calibration				
RB 1	0.56	0.03	15.46	1.91
RB 2	0.45	0.03	13.08	1.91
RB 3	0.49	0.03	12.15	1.91
RB 4	0.42	0.03	11.64	1.91
RB 5	0.39	0.03	11.60	1.91
RB 6	0.56	0.03	14.72	1.91
RB 7	0.55	0.03	16.53	1.91
RB 8	0.55	0.03	16.53	1.91
RB 9	0.58	0.03	16.89	1.91
RB 10	0.60	0.03	18.28	1.91
	Mean (µg/g)	± coeff. of variation %	Mean (µg/g)	± coeff. of variation %
RB	0.52	14.1	14.69	16.5
Glass standards and NMA calibration				
RB 1	0.43	0.03	10.92	1.91
RB 2	0.35	0.03	9.23	1.91
RB 3	0.38	0.03	8.57	1.91
RB 4	0.33	0.03	8.22	1.91
RB 5	0.30	0.03	8.19	1.91
RB 6	0.44	0.03	10.39	1.91
RB 7	0.43	0.03	11.67	1.91
RB 8	0.45	0.03	11.92	1.91
RB 9	0.45	0.03	11.92	1.91



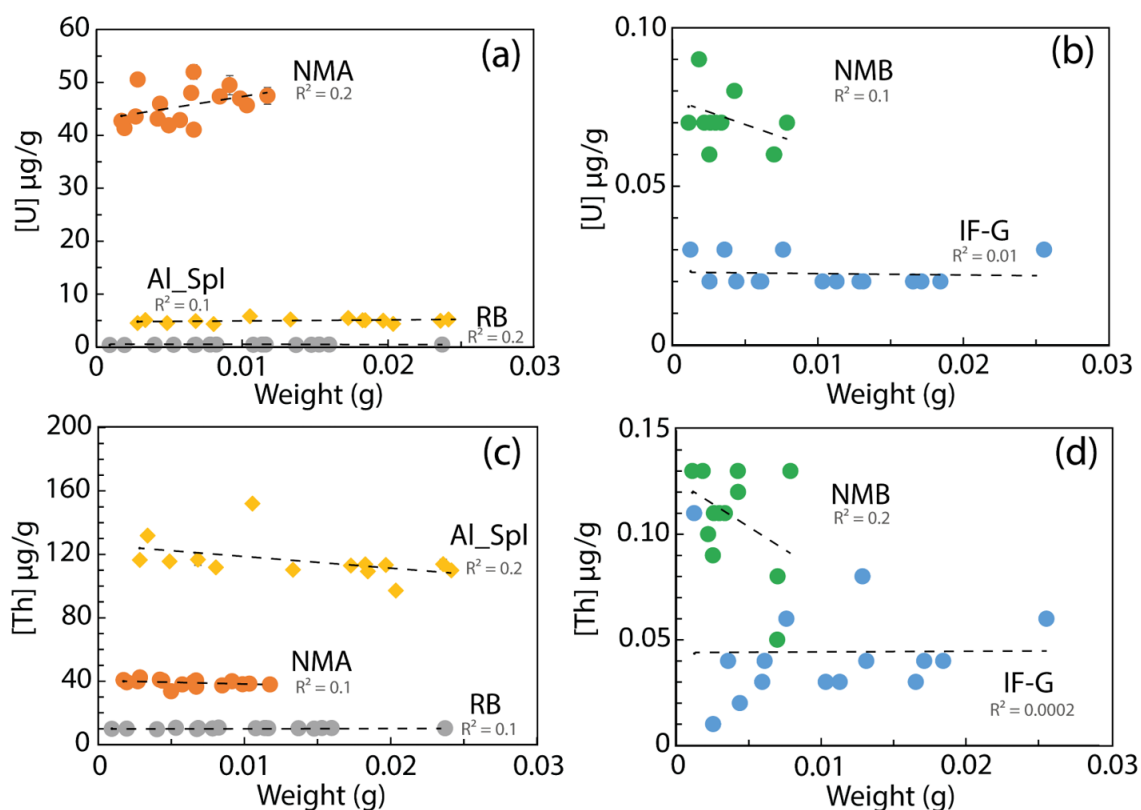
RB 10	0.46	0.03	12.90	1.91
	Mean (µg/g)	± coeff. of variation %	Mean (µg/g)	± coeff. of variation %
RB	0.40	14.3	10.39	16.7
Glass standards calibration				
Al_Spl 1	4.40	0.17	95.79	2.73
Al_Spl 2	3.66	0.17	86.31	2.73
Al_Spl 3	4.10	0.17	89.70	2.73
Al_Spl 4	3.45	0.17	71.76	2.73
Al_Spl 5	5.03	0.17	104.90	2.73
Al_Spl 6	3.46	0.17	87.72	2.73
Al_Spl 7	4.03	0.17	81.64	2.73
Al_Spl 8	4.53	0.17	92.07	2.73
Al_Spl 9	4.34	0.17	89.83	2.73
Al_Spl 10	3.47	0.17	88.65	2.73
	Mean (µg/g)	± coeff. of variation %	Mean (µg/g)	± coeff. of variation %
Al_Spl	4.05	13.3	88.84	9.7
Glass standards and NMA calibration				
Al_Spl 1	4.31	0.17	85.41	2.73
Al_Spl 2	3.58	0.17	76.96	2.73
Al_Spl 3	4.01	0.17	79.98	2.73
Al_Spl 4	3.38	0.17	63.98	2.73
Al_Spl 5	4.92	0.17	93.53	2.73
Al_Spl 6	3.38	0.17	78.21	2.73
Al_Spl 7	3.94	0.17	72.79	2.73
Al_Spl 8	4.43	0.17	82.09	2.73
Al_Spl 9	4.25	0.17	80.09	2.73
Al_Spl 10	3.40	0.17	79.04	2.73
	Mean (µg/g)	± coeff. of variation %	Mean (µg/g)	± coeff. of variation %
Al_Spl	3.96	13.3	79.21	9.7

4 Discussion

4.1 Dispersion of wet chemistry U-Th concentration values

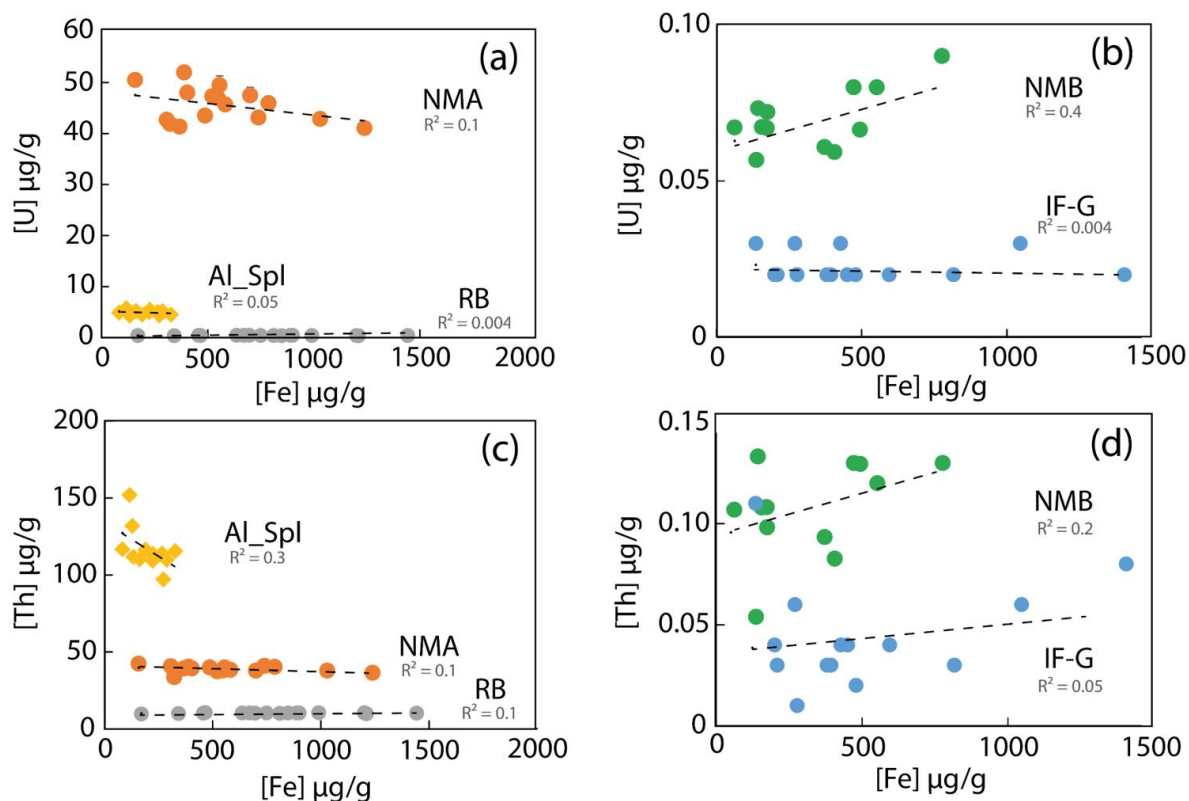
205 The U and Th concentrations measured for the four magnetite (IF-G, RB, NMA and NMB) and the aluminous spinel (Al_Spl) samples using wet chemistry extraction present contrasted values and different levels of dispersion (Figs. 1 and 2). The dispersion of U and Th concentrations could be linked to various parameters. Among them, we identified (i) the influence of the aliquot sample mass, (ii) an over dilution of sample during preparation or (iii) inherent heterogeneity of the U and Th distribution within the sample. Firstly, the possible impact of the aliquot mass on U and Th dispersion, has been

210 investigated by comparing the dispersion as a function of the sample mass as reported in Figure 4. Although slight dependency of U and Th concentrations on aliquot mass can be observed for some of the samples, statistically there is no obvious correlation between U - Th concentrations and aliquot mass.



215 **Figure 4.** U and Th concentration evolution with the mass of dissolved sample. (a) U concentration for NMA, Al_Spl and RB samples and (b) NMB and IF-G samples, (c) Th concentration for NMA, Al_Spl and (d) NMB and IF-G.

220 The impact of sample dilution and, thus, the effect of Fe concentration on the ICP-MS plasma were examined. U and Th contents are plotted against the Fe concentration in the analyzed solution on Figure 5. From one sample to another, the Fe content in solution varies from 62 to 1240 $\mu\text{g/g}$ corresponding to a dilution factor comprised between 400 and 5000. The effect of dilution (iron content) on the U and Th analysis precision, if any, cannot account for the dispersion of U and Th concentration. Moreover, under the analytical conditions indicated in §2.4.1., the limit of quantification was estimated to 0.5 ng/g . This implies that for a sample containing 0.1 $\mu\text{g/g}$ of U and Th (as for samples IF-G and NMB) and for dilution factors higher than 5000, the signal will be close to the quantification limit. Thus, when measuring magnetite or Al-spinel samples with a low concentration of U and Th, even if the dilution has no statistical effect on the dispersion results, the possibility of reaching concentration below quantification limit should be questioned.



225

Figure 5. U and Th concentrations as a function of iron concentration in the analyzed solution. (a) NMA, Al_Spl and RB and (b) NMB and IF-G samples. (c) NMA, Al_Spl and (d) NMB and IF-G.

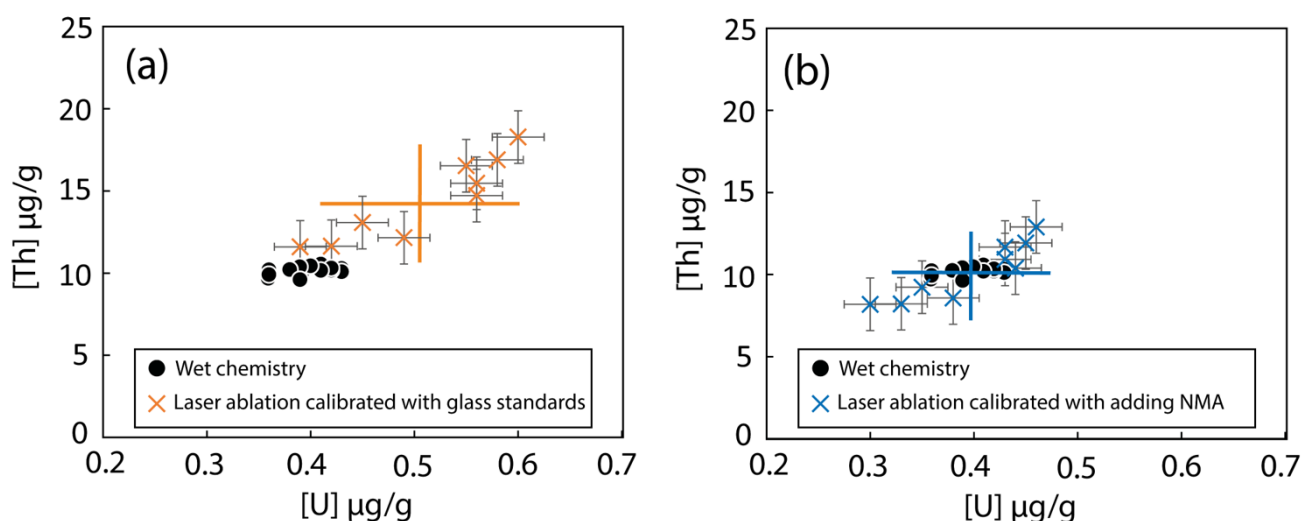
Finally, dispersion of U and Th contents could be associated with the chemical heterogeneity of the sample itself. The highest U and Th dispersion is encountered for samples, IF-G and NMB which bear the lowest U and Th contents (< 0.07 and $0.11 \mu\text{g/g}$ for U and Th respectively). Such a high U and Th dispersion for IF-G sample (20.2% and 56.8%, respectively) has been already reported in the literature as shown in Figure 1 and could be associated with the mineralogical heterogeneity of this sample. Nevertheless, NMB sample also yielded high dispersion (13.8% and 21.8% for U and Th respectively) compared to NMA sample (7.4% and 5.4% for U and Th respectively) even if the two samples have been prepared using exactly the same protocol. The only difference between these samples is the U and Th content; and we thus propose that the dispersion is merely due to concentration effect and the impossibility to measure precisely U and Th content for low value ($< 0.1 \mu\text{g/g}$) better than 20 %.

4.2 Accuracy of in situ laser ablation U and Th results

For magnetite samples, the U and Th concentrations obtained using laser ablation extraction method present different results as a function of the type of calibration that is used. For the RB sample, the U and Th concentration obtained using the silicate



240 glass standards yield values that are by 30% higher than the one obtained with the wet chemistry extraction method, as
shown on Figure 6a. However, with the addition of the NMA sample to the calibration, the U and Th concentration show
almost identical results to the wet chemistry method ($U=0.40\pm 0.03 \mu\text{g/g}$ and $Th=10.13\pm 0.26 \mu\text{g/g}$, Fig. 6b). Thus, we
propose to use NMA as standard. A cross-calibration by other laboratories will be the next step to certify the synthetic NMA
sample as a standard for U and Th concentration in magnetite. Furthermore, our synthesis protocol was successful in
245 obtaining nanomagnetite with low U and Th concentrations (NMB: $U\text{-}Th < 0.13 \mu\text{g/g}$). It is thus possible to extend the range
of U – Th concentration of the external synthetic nanomagnetite standard if needed.



250 **Figure 6.** Comparison between results obtained by LA-ICP-MS with two calibrations and by wet chemistry in the case of RB magnetite.
(a) Calibration with silicate glasses as mean value and dispersion reported with the orange crosses and (b) Calibration with addition of
NMA sample with mean value and associated dispersion (blue crosses). U and Th contents obtained using wet chemistry extraction
protocol are represented by the black dots.

Similarly, for Al_Spl sample, the U and Th concentrations obtained for the two types of calibrations are plotted in Figures 7a
and b and compared to the wet chemistry results. NMA addition to the calibration has no significant effect on the obtained U
255 which actually differs by more than 19% from the wet chemistry data. ($3.96\pm 0.53 \mu\text{g/g}$ using LA-ICP-MS and 4.94 ± 0.42
 $\mu\text{g/g}$ using wet chemistry, Figure 7). The Th concentrations obtained with LA-ICP-MS are systematically lower than the
concentrations obtained by wet chemistry ($116.01\pm 12.60 \mu\text{g/g}$) whatever the set of used standards ($79.21\pm 7.69 \mu\text{g/g}$ or
 $88.84\pm 8.63 \mu\text{g/g}$; Fig. 7). This is likely due to matrix effects, and it shows that even if magnetite and spinel *ss* are from the
same structural group (spinel), it is necessary to use a standard that is as close as possible in terms of mineral chemistry to
260 avoid systematic biases on the obtained results. It must be however noted that the precision on U and Th concentration
measurement with LA-ICP-MS is comparable to that achieved with the wet chemistry method. This is very encouraging for
the use of LA-ICP-MS to analyze U-Th content of spinel. Provided that appropriate standards are used, it is expected that
comparable precision and accuracy can be achieved with the two methods (laser ablation and wet chemistry), keeping in



mind that LA-ICP-MS data are much easier to collect in term of time and cost. The next step is therefore the production of appropriate U and Th Al-spinel standards.

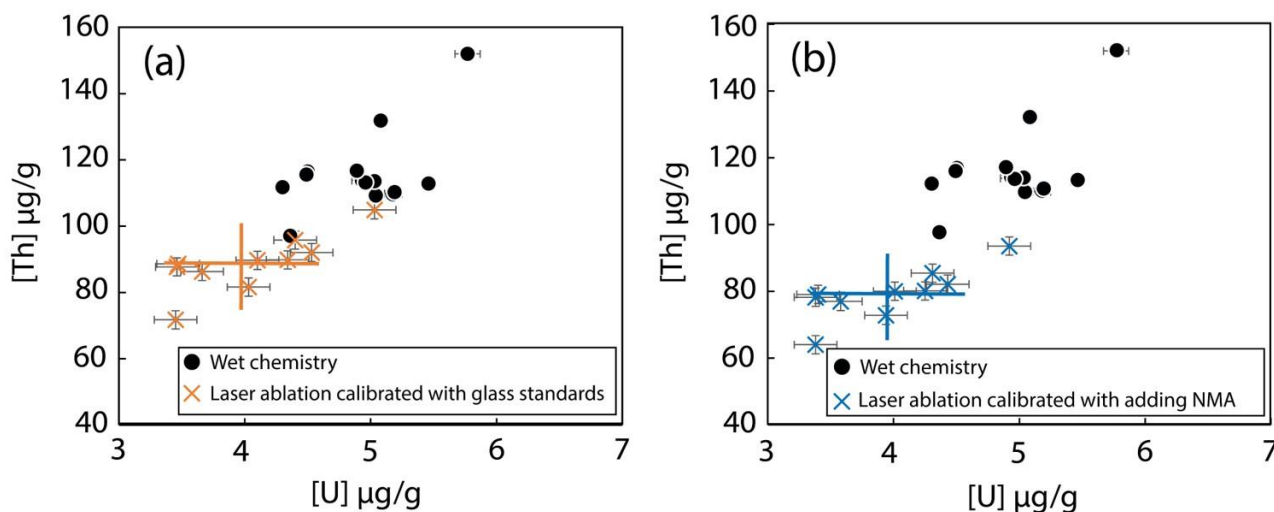


Figure 7. U and Th content obtained by wet chemistry and laser ablation method (a) Results obtained with silicate glass standards (orange crosses) and (b) with addition of NMA as standard (blue crosses). Wet chemistry data are represented by the black dots.

4.3 Implication for magnetite and spinel (U-Th)/He thermochronology

In the literature, MgHe dates dispersion ranges from 13 to 70% for crystals containing U and Th content below 0.1 µg/g (e.g., Cooperdock and Stockli 2016, Schwartz et al., 2020; Cooperdock et al., 2020), and is less than 5% for magnetite containing U and Th concentrations above 0.1 µg/g (Blackburn et al., 2007). Such dispersion includes the analytical errors on the He, U, Th and Sm measurement. Interestingly, the highest dates dispersion determined on natural magnetite with low U-Th content (<0.1 µg/g) is higher than the analytical one that can be estimated with the results of this study. For spinel, only one study exists with SpHe date dispersion of <9% (Cooperdock and Stockli, 2018). Indeed, dispersion on (U-Th)/He dates include the analytical errors on He, U and Th concentrations. If the amount of ⁴He is sufficient for a proper analysis with a noble gas mass spectrometer, the analytical error is <2% (e.g., Gautheron et al., 2021). In this study, we can estimate a dispersion on the MgHe date of ~24%, for crystals containing U and Th <0.1 µg/g, and of 4 to 10% for crystals with U and Th content > 0.4 µg/g. We simply propagate the error with a <2% for the He measurement, and dispersion on U and Th content knowing that they contribute at a different level to the He budget, where U and Th could be combined with the effective uranium (eU) content, with $eU = U + 0.238 \times Th + 0.0012 \times Sm$ (Cooperdock et al., 2019). The dispersion estimated here for MgHe dates, which is based on the analytical errors, is consistent with published dispersions associated with MgHe dating (Cooperdock and Stockli 2016; Schwartz et al., 2020; Cooperdock et al., 2020). For Al-spinel, we do not have enough samples to give statistical estimate, but a minimum error of 10% on the SpHe date for the determination of U and Th content > 5 µg/g is anticipated.



This study confirms that the error on the MgHe and SpHe dates are for a major part due to the difficulty to measure properly U and Th when their concentrations are lower than 0.01 $\mu\text{g/g}$. However, some published MgHe and SpHe data show a date dispersion that is higher than expected from the present study, which could be associated with alpha implantation from neighbor minerals, mineral inclusions, U-Th zoning, secondary growth of younger magnetite or different He diffusion behavior. Cooperdock and Stockli (2016) proposed a protocol to avoid the impact of alpha implantation from neighbor minerals and mineral inclusions by removing the outer crystal shell. Whereas Bassal et al. (2022) showed that He diffusion in magnetite is strongly affected by radiation damage induced by U and Th decay, with typical closure temperature ranging from 200 to 280°C depending on the damage dose and crystal size. As the U and Th content in magnetite crystals from the same geological case present similar values, poor MgHe date dispersion (<10%) associated with He diffusion changes is expected (Bassal et al., 2022). For spinel, no quantitative He diffusion coefficient is available limiting the interpretation of the origin of SpHe date dispersion.

In this study, the successful use of LA-ICP-MS with well-suited standards (NMA) opens the possibility to directly access the U and Th distribution across the whole grain for magnetite and spinel. As He content is determined on the bulk grain, if preliminary LA-ICP-MS data show that U and Th are homogeneously distributed in a magnetite grain, then, the MgHe will be estimated with dispersion at 20% if the U and Th content $>0.4 \mu\text{g/g}$. More generally, in-situ determination of U and Th in the magnetite or spinel crystals would allow to address the impact of U-Th zoning or secondary growing of magnetite with the alteration process. Finally, compared to wet chemistry methods, acquisition of precise (U-Th)/He dates by LA-ICP-MS may reveal easier, more time efficient, provided that certified and appropriate U - Th standard of magnetite and spinel are used.

305 **5 Conclusion**

U and Th concentrations ranging from 0.02 to 116.01 $\mu\text{g/g}$ have been determined in natural magnetite, synthetic U-Th doped magnetite and natural aluminous spinel for the purpose of (U-Th)/He thermochronology. This analytical investigation was based on the comparison of wet chemistry and in-situ laser ablation extraction methods considering their respective advantages and drawbacks. Firstly, we demonstrate that the highest U-Th dispersion is found for the samples with the lowest concentration. This high dispersion shows the difficulty with HR-ICP-MS analysis to measure U and Th concentrations below 0.1 $\mu\text{g/g}$ to better than 20%. This implies that magnetite and spinel (U-Th)/He thermochronological dating will yield data dispersion ranging from few percent for U- and/or Th-rich ($> 0.4 \mu\text{g/g}$) crystals and up to 20% for U-Th poor ($< 0.1 \mu\text{g/g}$) crystals. Moreover, this study highlights the importance of having new suitable magnetite and spinel standards to ensure accurate analysis of U and Th in oxides in wet chemistry and in-situ extraction. We show that the synthesis of minerals containing U and Th in controlled concentrations can be a way to produce homogeneous and suitable standards for wet chemistry and in-situ analyses.



The use of LA-ICP-MS with synthetic minerals is a promising tool for the acquisition of precise (U-Th)/He dates. Indeed, it allows investigating the distribution of U and Th within a given crystal and evidencing possible growth zones. Dating where U and Th concentration is determined by LA-ICP-MS, however, remains limited by the fact that He is measured on the whole grain or even on multiple grains. Those data can thus be used for dating only if the U-Th distribution is homogeneous in the studied crystals. The synthesis and characterization of U-Th doped-spinel standards is obviously a perspective of this work to access reliable U and Th measurement by wet chemistry and / or laser ablation methods.

Appendix A: Characterizations of U, Th doped synthetic nanomagnetite

Synthetic nanomagnetite NMA and NMB samples, are enriched in U-Th in the desired concentration range and predicted by our theoretical calculations. The synthesis protocol is presented in §2.1.2. The absence of U and Th in the remaining solutions was verified by analyzing these solutions with HR-ICP-MS at IUEM laboratory to ensure that all U and Th are incorporated into the nanomagnetite. In addition, two experiments were done with (i) desorption experiment to quantify the amount of sorbed U and Th sorbed on the surface, and (ii) pH steps dissolution experiment to calculate how much U-Th are sorbed on the surface or incorporated in the structure of the nanomagnetite. These two experiments allow to understand where U and Th are placed: sorbed at surface or present in the structure of nanomagnetite.

A1 Desorption of U-Th experiments

A first set of U-Th desorption experiments was performed on NMA sample. In a first step, U and Th are desorbed and kept in solution. In a second step, U-Th in solution are complexed in order to measure the complexes with UV-visible. In detail, according to Stopa and Yamaura (2010), U desorption can be achieved using Na_2CO_3 and Th can be desorbed using EDTA (Hunter et al., 1988). Two samples of magnetite standard (180 mg each) were therefore dipped in respectively 2 mL of 1.1 g/L Na_2CO_3 solution and 2 mL of 2.10^{-4} mol/L EDTA solution for 40 minutes with shaking. Samples, with U and Th in solution, were subsequently centrifuged at 13.4 rpm for 15 minutes. Then the concentrations of uranium or thorium in each supernatant were determined by complexing the U and Th by the Arsenazo III method at 650 nm using a UV-Vis spectrophotometer with a detection limit measured at $0.1\mu\text{g/L}$ (Yamaura et al., 2002). The UV-Vis result did not detect U-Arsenazo and Th-Arsenazo complexes. According to this experiment there are no U and Th sorbed on the surface of nanomagnetites. The U and Th, seems to be incorporated in the structure of nanoparticles.

A2 Dissolution of U-enriched-nanomagnetite during pH changes

A different experiment was set up to verify the results obtained by the complexation method (A1). This time, about two grams of nanomagnetite enriched with only $50\mu\text{g/g}$ of U were synthesized. After the rinsing step with oxygen-free MilliQ water, the U-doped magnetite was immediately suspended in a reactor containing 300 ml of 0.001 mol/l NaCl solution, previously deoxygenated for 30 min and kept under N_2 bubbling. The suspension was then subjected to decreasing pH steps



(8.5, 5.5, 4, 3, 2.3, 1.2 and 1) by addition of 0.1 and 1.5 mol/l HCl. At each step, the pH was kept constant for three hours by automatic addition of HCl using a Titrimetrohm 716 DMS instrument running Tiamo software. At the end of each pH
350 step, the suspension was sampled, centrifuged, and the supernatant was filtered at 0.20 μm . The Fe and U contents of the different pH-solutions were analyzed by ICP-MS at the Institut de Physique du Globe (France). This allows to follow the dissolution of uranium and iron according to the pH.

The expected pH of U sorption/desorption was modeled using PHREEQC Version 3 (Parkhurst and Appelo, 2013) using the surface complexation model of Missana et al. (2003) for a specific surface area approximated at 100 m^2/g . This pH is,
355 according to this model, is > 4 . If U is sorbed on the magnetite surface, solutions of pH 8.5 to 4 are expected to contain U. On the other hand, the expected pH of a magnetite dissolution is less than 4. Thus, if U is contained in the magnetite structure, solutions at pH 4 to 1 are expected to contain U. Based on the distribution of U in the solutions for each pH step, we can know at the end, the content of sorbed U and the content of U that is in the structure. According to our results, in solutions with pH > 5 there are no U in the solutions. In solutions with pH 5.5 and 4 there is 5% U and 2% Fe. From pH 3 to
360 1.2 there is 40% U and 20% Fe in solution and at pH 1: 55% U and 75% Fe are in solution. Thus, there is 5% of U sorbed on the surface of nanomagnetite. The majority (95%) of the U is incorporated in the structure of the nanomagnetite. We assume that Th behaves in a similar way.

Author contributions. MC collected and processed data, made figures, and contributed to the writing of the paper. S.S., F.B., AA, S.S. and C.G. initiated the study, processed data, and contributed to the writing of the paper. ML contributed to the
365 synthesize mineral process and contributed to the writing of the paper.

Competing interests. The authors declare that they have a possible conflict of interest as Cécile Gautheron is a member of the editorial board of the journal.

Acknowledgments. We thank Marie-Laure Rouget for helping to the calibrations of the ICP-MS and the LA-ICP-MS of IUEM. Rosella Pinna-Jamme (GEOPS) and Pierre Burkel (IPGP) are thanked for their help in the measurement of U and Th
370 content analysis of NMA. We thank Nathaniel Findling to helping for the characterization of our samples (SEM, XRD).

Financial support. This research has been supported by the Direction de l'Industrie, des Mines et de l'Environnement de Nouvelle Calédonie (DIMENC).



References

- 375 Bassal, F., Roques J., Corre, M., Brunet, F., Ketcham, R., Schwartz, S., Tassan-Got, L., and Gautheron, C.: Role of defects and radiation damage on He diffusion in magnetite: implication for (U-Th)/He thermochronology, *Minerals*, <https://doi.org/10.3390/min12050590>, 2022.
- Blackburn, T. J., Stockli, D. F., and Walker, J. D.: Magnetite (U-Th)/He dating and its application to the geochronology of intermediate to mafic volcanic rocks, *Earth Planet. Sci. Lett.*, 259, 360–371, <https://doi.org/10.1016/j.epsl.2007.04.044>, 2007.
- 380 Bolhar, R., Hofmann, A., Siah, M., Feng, Y. and Delvigne, C.: A trace element and Pb isotopic investigation into the provenance and deposition of stromatolitic carbonates, ironstones and associated shales of the ~3.0 Ga Pongola Supergroup, Kaapvaal Craton, *Geochim. Cosmochim. Acta*, 158, 57–78, <https://doi.org/10.1016/j.gca.2015.02.026>, 2015.
- Bolhar, R., Kamber, B. S., Moorbath, S., Fedo, C. M. and Whitehouse, M. J.: Characterisation of early Archaean chemical sediments by trace element signatures, *Earth Planet. Sci. Lett.*, 222, 43–60, <https://doi.org/10.1016/j.epsl.2004.02.0162004>,
385 2004.
- Cooperdock, E. H. G. and Ault, A. K.: Iron Oxide (U-Th)/He Thermochronology: New Perspectives on Faults, Fluids, and Heat, *Elements*, 16, 319–324, <https://doi.org/10.2138/gselements.16.5.319>, 2020.
- Cooperdock, E. H. G., Ketcham, R. A., and Stockli, D. F.: Resolving the effects of 2-D versus 3-D grain measurements on apatite (U-Th)/He age data and reproducibility, *Geochronology*, 1, 17–41, <https://doi.org/10.5194/gchron-1-17-2019>, 2019.
- 390 Cooperdock, E. H. G. and Stockli, D. F.: Unraveling alteration histories in serpentinites and associated ultramafic rocks with magnetite (U-Th)/He geochronology, *Geology* 44, 967–970, <https://doi.org/10.1130/G38587.1>, 2016.
- Cooperdock, E. H. G., Stockli, D. F., Kelemen, P. B., and Obeso, J. C.: Timing of Magnetite Growth Associated With Peridotite-Hosted Carbonate Veins in the SE Samail Ophiolite, Wadi Fins, Oman, *J. Geophys. Res.: Solid Earth* 125, <https://doi.org/10.1029/2019JB018632>, 2020.
- 395 Cooperdock, E. H. G. and Stockli, D. F.: Dating exhumed peridotite with spinel (U-Th)/He chronometry. *Earth and Planetary Science Letters* 489, 219–227, <https://doi.org/10.1016/j.epsl.2018.02.041>, 2018.
- Costa, M. M., Jensen, N. K., Bouvier, L. C., Connelly, J. N., Mikouchi, T., Horstwood, M. S. A., Suuronen, J. P., Moynier, F., Deng, Z., Agranier, A., Martin, L. A. J., Johnson, T. E., Nemchin, A. A., and Bizzarro, M.: The internal structure and geodynamics of Mars inferred from a 4.2-Gyr zircon record, *PNAS*, 117 (49), 30973–30979,
400 <https://doi.org/10.1073/pnas.2016326117>, 2020.
- Dulski, P.: Reference Materials for Geochemical Studies: New Analytical Data by ICP-MS and Critical Discussion of Reference Values, *Geostand. Geoanalytical Res.*, 25, 87–125, <https://doi.org/10.1111/j.1751-908X.2001.tb00790.x>, 2001.
- Gao, S., Liu, X., Yuan, H., Hattendorf, B., Günther, D., Chen, L., Hu, S.: Determination of Forty Two Major and Trace Elements in USGS and NIST SRM Glasses by Laser Ablation-Inductively Coupled Plasma-Mass Spectrometry.
405 *Geostandards Newsletter* 26, 181–196, <https://doi.org/10.1111/j.1751-908X.2002.tb00886.x>, 2002.



- Gautheron, C., and Zeitler, P. K.: Noble Gases Deliver Cool Dates from Hot Rocks: Elements, 16, 303–309, <https://doi.org/10.2138/gselements.16.5.303>, 2020.
- Gautheron, C., Hueck, M., Ternois, S., Heller, B., Schwartz, S., Sarda, P. and Tassan-Got, L.: Investigating the Shallow to Mid-Depth (>100–300 °C) Continental Crust Evolution with (U-Th)/He Thermochronology: A Review. Minerals 12, 563, 410 <https://doi.org/10.3390/min12050563>, 2022.
- Gautheron, C., Pinna-Jamme, R., Derycke, A., Ahadi, F., Sanchez, C., Haurine, F., Monvoisin, G., Barbosa, D., Delpech, G., Maltese, J., Sarda, P., and Tassan-Got, L.: Technical note: Analytical protocols and performance for apatite and zircon (U–Th)/He analysis on quadrupole and magnetic sector mass spectrometer systems between 2007 and 2020, Geochronology 3, 351–370, <https://doi.org/10.5194/gchron-3-351-2021>, 2021.
- 415 Govindaraju, K.: UPDATE (1984–1995) On Two Git - Iwg Geochemical Reference Samples: Albite From Italy, Al-I and iron formation sample from Greenland, IF-G, Geostand. Geoanalytical Res., 19, 55–96, <https://doi.org/10.1111/j.1751-908X.1995.tb00152.x>, 1995.
- Guilmette, C., Hébert, R., Wang, C., and Villeneuve, M.: Geochemistry and geochronology of the metamorphic sole underlying the Xigaze Ophiolite, Yarlung Zangbo Suture Zone, South Tibet, Lithos 112, 149–162, 420 <https://doi.org/10.1016/j.lithos.2009.05.027>, 2009.
- Hunter, K. A., Hawke, D. J., and Lee, K. C.: Equilibrium adsorption of thorium by metal oxides in marine electrolytes, Geochim. Cosmochim. Acta, 52, 627–636, [https://doi.org/10.1016/0016-7037\(88\)90324-9](https://doi.org/10.1016/0016-7037(88)90324-9), 1988.
- Inglis, E. C., Creech, J. B., Deng, Z., and Moynier, F.: High-precision zirconium stable isotope measurements of geological reference materials as measured by double-spike MC-ICPMS, Chem. Geol., 493, 544–552, 425 <https://doi.org/10.1016/j.chemgeo.2018.07.007>, 2018.
- Ilyinichna, O. O., Michailovich, L. S., Sergeevich, D. A., Gennadijevna, E. K.: An investigation of trace elements’ behavior during chemical preparation of ultramafic matrix rock samples using bomb digestion for analysis by ICP-MS, J. Anal. At. Spectrom, 35, 2627, 2020.
- Kamber, B. S., Bolhar, R., and Webb, G. E.: Geochemistry of late Archaean stromatolites from Zimbabwe: evidence for 430 microbial life in restricted epicontinental seas, Precambrian Res. 132, 379–399, <https://doi.org/10.1016/j.precamres.2004.03.006>, 2004.
- Koch, J., Feldmann, I., Jakubowski, N., and Niemax, K.: Elemental composition of laser ablation aerosol particles deposited in the transport tube to an ICP, Spectrochimica Acta Part B: Atomic Spectroscopy 57, 975–985, [https://doi.org/10.1016/S0584-8547\(02\)00021-6](https://doi.org/10.1016/S0584-8547(02)00021-6), 2002.
- 435 Kubik, E., Siebert, J., Blanchard, I., Agranier, A., Mahan, B., and Moynier, F.: Earth’s volatile accretion as told by Cd, Bi, Sb and Tl core–mantle distribution, Geochim. Cosmochim. Acta, 306, 263–280, <https://doi.org/10.1016/j.gca.2021.02.017>, 2021.



- Li, Z.-X. A. and Lee, C. T. A.: Geochemical investigation of serpentinized oceanic lithospheric mantle in the Feather River Ophiolite, California: Implications for the recycling rate of water by subduction, *Chem. Geol.*, 235, 161–185, 440 <https://doi.org/10.1016/j.chemgeo.2006.06.011>, 2006.
- Martínez-Mera, I., Espinosa-Pesqueira, M. E., Pérez-Hernández, R., and Arenas-Alatorre, J.: Synthesis of magnetite (Fe_3O_4) nanoparticles without surfactants at room temperature, *Materials Letters*, 61, 4447–4451, <https://doi.org/10.1016/j.matlet.2007.02.018>, 2007.
- Missana, T., Maffiotte, C., and García-Gutiérrez, M.: Surface reactions kinetics between nanocrystalline magnetite and 445 uranyl, *J. Colloid Interface Sci.*, 261, 154–160, [https://doi.org/10.1016/S0021-9797\(02\)00227-8](https://doi.org/10.1016/S0021-9797(02)00227-8), 2003.
- Parkhurst, D. L. and Appelo, C.A. J.: Description of Input and Examples for PHREEQC Version 3—A Computer Program for Speciation, Batch-Reaction, One-Dimensional Transport, and Inverse Geochemical Calculations U.S. Geological Survey, 2013.
- Parks, J., Lin, S., Davis, D. W., Yang, X.-M., Creaser, R. A., and Corkery, M. T.: Meso- and Neoproterozoic evolution of the 450 Island Lake greenstone belt and the northwestern Superior Province: Evidence from litho-geochemistry, Nd isotope data, and U–Pb zircon geochronology, *Precambrian Res.*, 246, 160–179, <https://doi.org/10.1016/j.precamres.2014.02.016>, 2014.
- Potin, S., Beck, P., Bonal, L., Schmitt, B., Garenne, A., Moynier, F., Agranier, A., Schmitt-Kopplin P., Malik, A. K., and Quirico, E.: Mineralogy, chemistry, and composition of organic compounds in the fresh carbonaceous chondrite Mukundpura: CM1 or CM2? *Meteorit. Planet. Sci.*, 55, 1681–1696, <https://doi.org/10.1111/maps.13540>, 2020.
- 455 Schwartz, S., Gautheron C., Ketcham R. A., Brunet F., Corre M., Agranier A., Pinna-Jamme R., Haurine F., Guéguen B., Monvoin G., and Riel N.: Unraveling the exhumation history of high-pressure ophiolites using magnetite (U-Th-Sm)/He thermochronometry, *Earth Planet. Sci. Lett.*, 543, 116359, <https://doi.org/10.1016/j.epsl.2020.116359>, 2020.
- Steenstra, E. S., Berndt, J., Klemme, S., and van Westrenen, W.: LA-ICP-MS analyses of Fe-rich alloys: quantification of 460 matrix effects for 193 nm excimer laser systems, *J. Anal. At. Spectrom.*, 34, 222–231, <https://doi.org/10.1039/C8JA00291F>, 2019.
- Stopa, L.C.B. and Yamaura, M.: Uranium removal by chitosan impregnated with magnetite nanoparticles: adsorption and desorption. *International Journal of Nuclear Energy Science and Technology* 5, 283, <https://doi.org/10.1504/IJNEST.2010.035538>, 2010.
- Tricart, P. and Schwartz, S.: A north-south section across the Queyras Schistes lustrés (Piedmont zone, Western Alps): Syn- 465 collision refolding of a subduction wedge, *Eclogae Geol. Helv.*, 99, 429–442, <https://doi.org/10.1007/s00015-006-1197-6>, 2006.
- Van Kooten, E. M. M. E., Moynier, F., and Agranier, A.: A unifying model for the accretion of chondrules and matrix, *PNAS*, 116 (38), 18860–18866, <https://doi.org/10.1073/pnas.1907592116>, 2019.
- Viehmann, S., Bau, M., Bühn, B., Dantas, E. L., Andrade, F. R. D., and Walde, D. H. G.: Geochemical characterisation of 470 Neoproterozoic marine habitats: Evidence from trace elements and Nd isotopes in the Urucum iron and manganese formations, Brazil, *Precambrian Res.*, 282, 74–96, <https://doi.org/10.1016/j.precamres.2016.07.006>, 2016.



Yamaura, M., Wada, L. Y., and Ribeiro, F. C.: Spectrophotometric determination of uranium (VI) with arsenazo III in a nitric medium; Determinação espectrofotométrica de urânio (VI) com arsenazo III, em meio nítrico, p. Medium: X; Size: 5 pages. Associação Brasileira de Energia Nuclear, Rio de Janeiro, RJ (Brazil), 2002.